RESEARCH ARTICLE
doi: 10.2306/scienceasia1513-1874.2024.002

ScienceAsia 50 (1): 2024: ID 2024002: **1–7**

A sufficient descent conjugate gradient method for impulse noise removal

Peiting Gao, Yongfei Wu*

College of Data Science, Taiyuan University of Technology, Shanxi 030024 China

*Corresponding author, e-mail: wuyongfei@tyut.edu.cn

Received 21 Apr 2022, Accepted 25 Mar 2023
Available online 16 Jan 2024

ABSTRACT: In this paper, we introduce a modified PRP-type conjugate gradient (CG) method for impulse noise removal in the second phase of the two-phase method. A nice property of the scheme is that the search direction at each iteration satisfies the sufficient descent condition independent of any line search. Under the Armijo-type line search, its global convergence result is proved. Numerical comparison is given to illustrate that the proposed method for removing impulse noise is promising.

KEYWORDS: image processing, variational method, two-phase method, conjugate gradient method, global convergence

MSC2020: 65K05 90C30 90C06

INTRODUCTION

Image processing is a highly diverse field which includes subfields such as image recognition, image segmentation, and image denoising [1, 2]. Image denoising is a typical inverse problem and is hard to be solved. A common type of noise in images is the impulse noise which can be further categorized the two types: salt-and-pepper noise, for which the noisy pixels can take only the maximal and minimal pixel values, and the random-valued noise, for which the noisy pixels can take any random values between the maximal and minimal pixel values.

Numerous methods for restoring images corrupted by impulse noise have been proposed in past years. Among these methods, two methods are the most popular among research activities. One is the median filter and its several remedies [3–5] which are based on nonlinear digital filters [6]. However, its performance is not good when the noise level is high since they always fail to obtain local image features such as the possible presence of edges. Another is variational method [7], which is depended on variational framework and is capable of preserving the details and the edges. But, these methods change the gray level of each pixel including uncorrupted ones.

In order to avoid the disadvantages of the methods mentioned above, Chan et al [8] proposed a two-phase method based on the adaptive median filter method (AMF) [3] and the variational method [7, 9, 10]. More precisely, the noise pixels are first detected by using AMF method and then they are restored by minimizing an objective function $\mathscr{G}_\alpha$ with an ℓ_1 data-fitting term and a regularization term involving an edge-preserving potential function $\varphi_\alpha(t)$ [8]. The objective function $\mathscr{G}_\alpha$ is computed as follows:

$$\mathscr{G}_\alpha(u) = \sum_{(i,j)\in\mathscr{G}} \left\{ |u_{i,j} - y_{i,j}| + \frac{\beta}{2} \sum_{(m,n)\in\mathscr{V}_{i,j}\setminus\mathscr{N}} 2\varphi_\alpha\left(u_{i,j} - y_{m,n}\right) \right\} + \frac{\beta}{2} \sum_{(i,j)\in\mathscr{G}} \left\{ \sum_{(m,n)\in\mathscr{V}_{i,j}\bigcap\mathscr{N}} \varphi_\alpha(u_{i,j} - u_{m,n}) \right\}, \quad (1)$$

where $\mathscr{N} \subset \mathscr{A}$ is the set of the noisy candidates, which are detected by AMF method in the first phase, $\mathscr{A} = \{1, 2, 3, \ldots, M\} \times \{1, 2, 3, \ldots, N\}$ is the index set of $\mathbf{X}$ denoting the original image with M-by-N pixels, $\mathscr{V}_{i,j}$ is the set of the four closest neighbors of the pixels at the position $(i, j) \in \mathscr{A}$, $y_{i,j}$ is the observed pixel value of the image at the position (i, j), β is the regularization parameter, $u = [u_{i,j}]_{i,j\in\mathscr{N}}$ is a column vector of length c ordered lexicographically with c denoting the number of elements of $\mathscr{N}$, and φ_α is an edge-preserving function.

Because of introducing the regularization term involving pertinent prior information, the two-phase method can preserve the details and the edges of the image and unchange the uncorrupted pixels. However, the objective function $\mathscr{G}_\alpha$ to be minimized is nonsmooth as it includes a nonsmooth ℓ_1 data-fitting term, and so it is destined to the high cost of getting the minimizer. In order to overcome the drawbacks, Chan et al [11] proved that the nonsmooth ℓ_1 data-fitting term can be dropped because it is useless in the second phase. The objective function $\mathscr{G}_\alpha(1)$ is converted to $\mathscr{F}_\alpha(2)$ as follows:

$$\mathscr{F}_\alpha(u) = \sum_{(i,j)\in\mathscr{G}} \left\{ \sum_{(m,n)\in\mathscr{V}_{i,j}\setminus\mathscr{N}} \varphi_\alpha\left(u_{i,j} - y_{m,n}\right) \right\} + \frac{1}{2} \sum_{(i,j)\in\mathscr{G}} \left\{ \sum_{(m,n)\in\mathscr{V}_{i,j}\bigcap\mathscr{N}} \varphi_\alpha(u_{i,j} - u_{m,n}) \right\}. \quad (2)$$

Despite minimizing $\mathscr{F}_\alpha$ instead of $\mathscr{G}_\alpha$ in the second phase, the quality of the restored images is not affected. Some related results are showed in [12, 13]. Thus, the 2-phase method for impulse noise removal can be viewed as a minimization unconstrained optimization problem of the new objective function $\mathscr{F}_\alpha$. Numerous methods have been proposed by authors to minimize $\mathscr{F}_\alpha$. Besides, Yin et al [14] recently proposed a generalized hybrid conjugate gradient projection method-based algorithm to restore image by solving large-scale convex constrained equations.

In this paper, we are interested in the conjugate gradient (CG) type method for minimizing the new objective function $\mathscr{F}_\alpha$. Yu et al [15] introduced a descent spectral CG method for impulse noise removal, in which the search direction is descent with $C \geqslant 1/4$. Recently, Liu et al [9] suggested a modified three term PRP-type CG method for removing impulse noise, in which the search direction satisfies the sufficient descent condition by $r \geqslant 0$. For the above-mentioned methods, the search direction satisfies the sufficient descent condition with some extra restrictions, which may lead to bad results. Hence, developing the search direction satisfies the sufficient descent condition without any restriction is significative.

As far as we know, Cheng [16] proposed a modified PRP-type CG method for solving unconstrained optimization problems. An attractive feature of the proposed method is that the search direction obtained satisfies the sufficient descent condition regardless of any restriction. Motivated by [9] and [16], we introduced a descent PRP-type CG method in which the search direction generated at each iteration is sufficient descent without any restriction. In numerical experiments, we employ the salt-and-pepper noise and $\varphi_\alpha(t)$ is defined by the Huber function [17]. The preliminary numerical results show that the proposed method outperforms other competitors to remove salt-and-pepper noise.

ALGORITHM

In this section, we first review a general formula of CG method and the related works. Then, we present a modified PRP CG method for minimizing $\mathscr{F}_\alpha$. In what follows, all vectors are column vectors, $\|\cdot\|$ is denoted by the Euclidian norm and the superscript $\top$ indicates transposition.

Because of its simplicity and low memory requirements, the nonlinear CG methods have been applied to solve unconstrained optimization problem:

$$\min f(x), \qquad x \in \mathbb{R}^n, \tag{3}$$

where $f : \mathbb{R}^n \to \mathbb{R}$ is a continuously differentiable function, $g(x_k) = g_k = \nabla f(x_k)$ and it is the gradient of the objective function f at the point x_k. A conjugate gradient method generates a sequence of iterative points $\{x_k\}$ described by

$$x_{k+1} = x_k + \alpha_k d_k, \qquad k = 0, 1, \dots,$$

where x_k is the k-th iterative point, $\alpha_k > 0$ is called the stepsize, and d_k is search direction computed by

$$d_0 = -g_0, \quad d_k = -g_k + \beta_k d_{k-1}, \qquad k = 1, 2, \dots,$$

where β_k is a scalar parameter. In this paper, we focus on the famous Polak-Ribiére-Polyak (PRP) method [18, 19] in which β_k is computed by

$$\beta_k^{\mathrm{PRP}} = \frac{g_k^\top y_{k-1}}{\|g_{k-1}\|^2},$$

with $y_{k-1} = g_k - g_{k-1}$. By the Gram-Schmidt orthgonalization, Cheng [16] introduced a CG method based on PRP method and the search direction is defined as:

$$d_k = -g_k + \beta_k^{\mathrm{PRP}} d_{k-1} - \beta_k^{\mathrm{PRP}} \frac{g_k^\top d_{k-1}}{\|g_k\|^2} g_k.$$

A nice property is that such defined direction d_k satisfied sufficient descent condition independent of any line search.

Recently, Liu et al [9] proposed a three-term CG method involving the modified PRP CG method as follows:

$$d_k = -g_k + \beta_k^{\mathrm{mPRP}} d_{k-1} + \theta_k y_{k-1}, \tag{4}$$

where $\beta_k^{\mathrm{mPRP}} = \frac{1}{\|g_{k-1}\|^2}\left(y_{k-1} - \frac{r\|y_{k-1}\|^2 d_{k-1}}{\|g_{k-1}\|^2}\right)^\top g_k$, $\theta_k = -\frac{g_k^\top d_{k-1}}{\|g_{k-1}\|^2}$, and $r \geqslant 0$. They proved that this method satisfies the sufficient descent condition with $r \geqslant 0$. Observe that if $r < 0$, this search direction may generate an ascent direction.

Motivated by the above articles, we consider a modified PRP CG method such that the search direction is generated by the following way:

$$d_k = -g_k + \beta_k^{\mathrm{mPRP}} d_{k-1} - \beta_k^{\mathrm{mPRP}} \frac{g_k^\top d_{k-1}}{\|g_k\|^2} g_k, \tag{5}$$

Notice that such defined direction d_k satisfies the sufficient descent condition at each iteration without $r \geqslant 0$. Obviously,

$$g_k^\top d_k = -\|g_k\|^2. \tag{6}$$

Furthermore, we obtain that

$$\|g_k\| \leqslant \|d_k\|.$$

Next, we list the detailed process of Algorithm 1 based on the above analysis.

Algorithm 1

Step 0. Given an initial point $x_0 \in \mathbb{R}^n$, and $0 < \rho < 1$, $\sigma > 0$, and $\tau > 0$. Set $k = 0$.

Step 1. If the stopping criteria holds, stop. Otherwise go to Step 2.

Step 2. Compute the direction d_k as follows:

- If $k=0$, then $d_k=-g_k$.
- If $k>0$, then

$$d_k=-g_k+\beta_k^{\mathrm{mPRP}}d_{k-1}-\beta_k^{\mathrm{mPRP}}\frac{g_k^\top d_{k-1}}{\|g_k\|^2}g_k,$$

where

$$\beta_k^{\mathrm{mPRP}}=\frac{1}{\|g_{k-1}\|^2}\left(y_{k-1}-\frac{r\|y_{k-1}\|^2 d_{k-1}}{\|g_{k-1}\|^2}\right)^\top g_k, \quad (7)$$

and r is a constant.

Step 3. Set $x_{k+1}=x_k+\alpha_k d_k$, when the step-size α_k is computed by using the following technique based on the Armijo line search, that is $\alpha_k=t_k\rho^i$, with i being the smallest nonnegative integer such that

$$-f(x_k+\alpha_k d_k)\leqslant f(x_k)-\sigma\alpha_k^2\|d_k\|^2, \quad (8)$$

where $t_k=\min\{\tau\|g_k\|^2/\|d_k\|^2,1\}$.

Step 4. Set $k:=k+1$, go to Step 1.

GLOBAL CONVERGENCE ANALYSIS

In this section, the global convergence of Algorithm 1 is established and the following assumption is needed.

Assumption 1

(i) The level set $\Lambda=\{X|f(X)\leqslant f(X_0)\}$ is bounded.

(ii) In some neighborhood $\tilde{N}$ of Ω, the objective function f is continuously differentiable and its gradient g is Lipschitz continuous in $\tilde{N}$, i.e., there exists a constant $L>0$ such that

$$\|g(x)-g(y)\|\leqslant L\|x-y\|, \quad \forall x,y\in\tilde{N},$$

which imply that there exists a positive constant γ so that

$$\|g(x)\|\leqslant\gamma, \qquad \forall x\in\tilde{N}.$$

Lemma 1 *Let Assumption 1 hold, and the sequence $\{d_k\}$ be generated by Algorithm 1, then the sequence $\{\|d_k\|\}$ is bounded.*

Proof: By Eq. (7), we have

$$\begin{aligned}\left|\beta_k^{\mathrm{mPRP}}\right| &\leqslant \frac{1}{\|g_{k-1}\|^2}|g_k^\top y_{k-1}|+\frac{|r|\|y_{k-1}\|^2|g_k^\top d_{k-1}|}{\|g_{k-1}\|^4}\\ &\leqslant \frac{1}{\|g_{k-1}\|^2}\|g_k\|\|y_{k-1}\|+\frac{|r|\|y_{k-1}\|^2\|g_k\|\|d_{k-1}\|}{\|g_{k-1}\|^4}. \quad (9)\end{aligned}$$

By (9) and the Assumption 1, we obtain

$$\begin{aligned}\|d_k\| &\leqslant \|g_k\|+2\left|\beta_k^{\mathrm{mPRP}}\right|\|d_{k-1}\|\\ &\leqslant \|g_k\|+2\left(\frac{\|g_k\|\|y_{k-1}\|}{\|g_{k-1}\|^2}+\frac{|r|\|y_{k-1}\|^2\|d_{k-1}\|\|g_k\|}{\|g_{k-1}\|^4}\right)\|d_{k-1}\|\\ &\leqslant \|g_k\|+\frac{2\|y_{k-1}\|\|d_{k-1}\|}{\|g_{k-1}\|^2}\|g_k\|+\frac{2|r|\|y_{k-1}\|^2\|d_{k-1}\|^2\|g_k\|}{\|g_{k-1}\|^4}\\ &\leqslant \|g_k\|+\frac{2L\alpha_{k-1}\|d_{k-1}\|^2}{\|g_{k-1}\|^2}\|g_k\|+\frac{2|r|L^2\alpha_{k-1}^2\|d_{k-1}\|^4}{\|g_{k-1}\|^4}\|g_k\|\\ &\leqslant \|g_k\|+2L\tau\|g_k\|+2|r|L^2\tau^2\|g_k\|\\ &=\left(1+2L\tau+2|r|L^2\tau^2\right)\|g_k\|\\ &\leqslant (1+2L\tau+2|r|L^2\tau^2)\gamma.\end{aligned}$$

Due to $d_0=-g_0$, we have $\|d_0\|\leqslant\gamma$. Then, the sequence $\|d_k\|$ generated by Algorithm 1 is bounded. □

Lemma 2 *Let Assumption 1 hold, and the sequence $\{d_k\}$ be generated by Algorithm 1, then we have*

$$\lim_{k\to\infty}\alpha_k^2\|d_k\|^2=0.$$

Proof: By (8), we have

$$\sigma\alpha_k^2\|d_k\|^2\leqslant f(x_k)-f(x_{k+1}) \quad (10)$$

By adding (10), the above equations for $k=0,1,2,\dots$, we obtain

$$\sigma\sum_{k=0}^{\infty}\alpha_k^2\|d_k\|^2\leqslant\sum_{k=0}^{\infty}(f(x_k)-f(x_{k+1}))\leqslant f(x_0)<\infty.$$

which mean that

$$\lim_{k\to\infty}\alpha_k^2\|d_k\|^2=0.$$

□

Theorem 1 *Let Assumption 1 hold, and the sequence $\{d_k\}$ be generated by Algorithm 1, then the conclusion holds that*

$$\liminf_{k\to\infty}\|g_k\|=0.$$

Proof: If

$$\liminf_{k\to\infty}\alpha_k>0,$$

by (6), Lemma 1 and Lemma 2, we obtain that

$$\liminf_{k\to\infty}\|g_k\|=0.$$

If

$$\liminf_{k\to\infty}\alpha_k=0,$$

there exists an infinite index set K so that

$$\liminf_{k\in K,k\to\infty}\alpha_k=0.$$

From the definition of α_k, we can find that $\rho^{-1}\alpha_k$ does not satisfy the line search and the inequality holds as follows:

$$f(x_k+\rho^{-1}\alpha_k d_k) > f(x_k) - \delta\rho^{-2}\alpha_k^2\|d_k\|^2. \tag{11}$$

By Assumption 1, we get that

$$\begin{aligned}
& f(x_k+\rho^{-1}\alpha_k d_k) - f(x_k) \\
&= \int_0^1 g(x_k+t\rho^{-1}\alpha_k d_k)^\top(\rho^{-1}\alpha_k d_k)\,\mathrm{d}t \\
&= \int_0^1 [g(x_k+t\rho^{-1}\alpha_k d_k) - g(x_k)]^\top](\rho^{-1}\alpha_k d_k)\,\mathrm{d}t \\
&\quad + \rho^{-1}\alpha_k g_k^\top d_k \\
&\leqslant \frac{1}{2}L\rho^{-2}\alpha_k^2\|d_k\|^2 + \rho^{-1}\alpha_k g_k^\top d_k \\
&= \frac{1}{2}L\rho^{-2}\alpha_k^2\|d_k\|^2 - \rho^{-1}\alpha_k\|g_k\|^2.
\end{aligned} \tag{12}$$

Combining (12) with (6) and (11), we obtain that

$$\|g_k\|^2 \leqslant \rho^{-1}\left(\frac{1}{2}L+\delta\right)\alpha_k\|d_k\|^2.$$

Due to Lemma 1, Lemma 2 and

$$\liminf_{k\to\infty}\alpha_k = 0,$$

we have

$$\lim_{k\to\infty}\|g_k\| = 0.$$

To sum up, the conclusion holds. □

Remark 1 According to [13, Proposition 1], the $\mathscr{F}_\alpha$ is smooth when φ_α is smooth. In this paper, the edge-preserving potential function is defined as the Huber function:

$$\varphi_\alpha = \begin{cases} \frac{t^2}{2\alpha}, & \text{if } |t| \leqslant \alpha, \\ |t| - \frac{\alpha}{2}, & \text{otherwise,} \end{cases} \tag{13}$$

where $\alpha > 0$. Obviously, $\mathscr{F}_\alpha$ is continuously differentiable, convex, and its gradient ∇F_α is first order Lipschitz continuous. Furthermore, the global minimum of $\mathscr{F}_\alpha$ exists. Interested readers may refer to [9, Propositions 1–3]. Hence, Algorithm 1 can be used for restoring the images corrupted by impulse noise, which has some nice features, such as simplicity, sufficient descent direction without any restriction, and global convergence.

Remark 2 To minimize $\mathscr{F}_\alpha$ by Algorithm 1, we view $\mathbf{u}$ as a column vector of length c lexicographically, in which c is the number of elements of $\mathscr{N}$. In fact, $\mathscr{F}_\alpha$ can be viewed as a special case of the problem (3), thus, Algorithm 1 proposed for the problem (3) is reasonable.

NUMERICAL PERFORMANCE

In this section, we presented the results of a series of experiments to illustrate the performance of Algorithm 1 for removing the salt-and pepper impulse noise and compare its performance with existing state-of-the-art algorithm, including the three-term PRP conjugate method (referred as TPRP) [9]. The edge-preserving potential function $\varphi_\alpha(t)$ is the Huber function (13) with $\alpha = 10$. All experiments were implemented under MATLAB (Version 2017b) environment and run on a PC with 2.30 GHZ CPU processor and 8.0 GB memory.

In the experiments, we choose Lena (256 × 256), Cameraman (256 × 256), Barbara (512 × 512) and Baboon (512 × 512) as the test images. Herein, the peak signal noise ratio (PSNR) [20] is calculated to quantify image quality upgradation after denoising procedure, and the formula is defined as

$$\mathrm{PSNR} = 10\log_{10}\frac{(N-1)^2}{\frac{1}{MN}\sum_{i,j}(u_{i,j}^* - x_{i,j})^2}.$$

In order to compare the effectiveness of the test method fairly, the line search and the parameters involved for competing method is from the original paper. In this paper, the parameter in Algorithm 1 are chosen by betting the best PSNR values as follows: $\sigma = 0.5$, $\rho = 0.5$ and $\tau = \frac{\sqrt{99}}{8}$. The stopping criteria of the minimization are

$$\frac{|F(\mathbf{u}_k) - F(\mathbf{u}_{k-1})|}{F(\mathbf{u}_k)} \leqslant \varepsilon \quad \text{or} \quad \frac{\|\mathbf{u}_k - \mathbf{u}_{k-1}\|}{\|\mathbf{u}_k\|} \leqslant \varepsilon,$$

where $\epsilon = 10^{-4}$.

In this section, the numerical comparison were conducted from two aspects. Firstly, we discuss the parameter r in Algorithm 1 to obtain an acceptable image restoration results. Therefore, we choose different r to test the effectiveness of Algorithm 1. The detailed numerical results are summarized in Table 1, which is presented in the form "NI/CPU/PSNR". "Niter" stands for the number of iterations, "CPU" stands for the CPU time required for the whole image denoising process, and "NL" stands for the noise level. Table 1 shows that Algorithm 1 performs best when the parameter $r = 0$. Secondly, we investigate the computational efficiency of TPRP method. The experiments are showed for the average results from five different noise samples of each image at each noise level. The results are listed in Table 1. From Table 1, it is not difficult to obtain that Algorithm 1 can successfully remove noise with ($r = -1$), and TPRP method ($r \geqslant 0$) cannot be used to deal with it. Then from Table 1, data format in Table 2 is consistent with that in Table 1. "Niter", "CPU" and "PSNR" all stand for the average of the corresponding data in Table 2. Table 2 indicates that Algorithm 1 ($r = 0$) has absolute advantages in the

Table 1 The results of the salt-and pepper noise removal via Algorithm 1 with different r.

Image	NL	$r=-1$	$r=0$	$r=1$
		NI/CPU/PSNR	NI/CPU/PSNR	NI/CPU/PSNR
Lena	0.3	38/0.9442/39.5604	33/0.86/39.4508	37/0.9340/39.3387
	0.5	53/1.6181/36.2405	50/1.52533/36.1649	53/1.6006/36.0527
	0.7	72/2.1859/32.9788	69/2.1123/33.1216	80/2.1132/33.0879
	0.9	163/3.1796/28.7250	148/2.8831/28.7093	163/3.1784/28.9564
Cameraman	0.3	58/1.3671/36.7560	54/1.2829/36.6279	56/1.3159/36.4710
	0.5	70/2.0705/33.4324	68/2.0121/33.3550	68/2.0124/33.0973
	0.7	94/2.5934/30.6907	93/2.4613/31.0721	96/2.5073/30.6286
	0.9	179/3.6216/27.2220	178/3.6011/27.3443	188/3.5604/27.2268
Barbara	0.3	38/3.7640/35.0806	37/3.6570/35.1309	38/3.7061/35.1333
	0.5	49/6.8907/32.4663	46/6.5241/32.4430	47/6.5971/32.4321
	0.7	65/9.2749/30.6253	62/8.6846/30.6137	64/8.8865/30.5832
	0.9	128/16.2696/28.5597	126/16.0954/28.5945	126/16.1282/28.5325
Baboon	0.3	41/4.0800/33.4618	41/3.9914/33.4610	41/4.1958/33.4452
	0.5	52/7.2834/30.6219	51/7.2434/30.6342	53/7.4044/30.6004
	0.7	72/9.7734/28.3937	69/9.4710/28.4093	73/9.8339/28.4142
	0.9	124/19.9708/26.3612	120/18.2438/26.3470	127/18.9068/26.3780

Table 2 The results of the salt-and pepper noise removal via TPRP method Algorithm 1 ($r=0$).

Image	NL	TPRP method	Algorithm 1 ($r=0$)
		NI/CPU/PSNR	NI/CPU/PSNR
Lena	0.3	44/1.0767/39.1855	33/0.8764/39.2185
	0.5	50/1.5559/36.1226	46/1.4669/36.0134
	0.7	84/2.2515/33.0647	73/1.9696/33.1343
	0.9	153/3.0341/28.4516	139/2.8404/28.7287
Cameraman	0.3	62/1.4605/36.4940	52/1.2778/36.5752
	0.5	72/2.1133/33.6533	68/2.0466/33.5211
	0.7	97/2.5047/30.4425	88/2.5140/30.7138
	0.9	176/3.3631/27.1365	147/3.0963/27.2260
Barbara	0.3	39/4.1143/35.1078	37/3.9403/35.0755
	0.5	49/7.7791/32.4582	47/7.5141/32.4067
	0.7	64/10.0530/30.6405	62/10.1097/30.6096
	0.9	125/18.5569/28.5923	120/17.3208/28.5258
Baboon	0.3	42/4.6022/33.4330	40/4.2608/33.4442
	0.5	52/7.9431/30.5748	49/7.1642/30.6334
	0.7	71/11.3374/28.4237	66/9.5323/28.4001
	0.9	125/18.2859/26.3308	120/18.6282/26.3493

number of iterates and the CPU time, and it performs best in removing the salt-and-pepper impulse noise for most cases. Fig. 1 shows the flow chart of our experiments. Fig. 2 gives that the restoration results via TPRP method and Algorithm 1 ($r=0$) for the test images corrupted with 0.7 salt-and-pepper noise.

CONCLUSION

In this paper, we propose an efficient conjugate gradient method for impulse noise removal. An attractive feature of the proposed method is that the search direction obtained satisfies the sufficient descent condition regardless of any restriction. And its global convergence is proved under Armijo-type line search. Numerical comparison is given to illustrate that the proposed method ($r=0$) for removing impulse noise is promising and robust. Furthermore, in the Numerical comparison section, we successfully use Algorithm 1 to remove noise with ($r=-1$), and TPRP method ($r \geqslant 0$) cannot be used to deal with it. In this paper, r is a constant and we try to construct different r to satisfy different conditions to improve computational efficiency in future.

Acknowledgements: This research was supported by the National Science Foundation of Shanxi Province, China (No. 202203021212255) and the National Natural Foundation of China (No. 61901292).

REFERENCES

1. Wu YF, Li M, Zhang QF, Liu Y (2018) A Retinex modulated piecewise constant variational model for image segmentation and bias correction. *Appl Math Model* **54**, 697–709.
2. Zeng C, Wu C, Jia R (2019) Non-Lipschitz models for image restoration with impulse noise removal. *SIAM J Imaging Sci* **12**, 420–458.
3. Hwang H, Haddad RA (1995) Adaptive median filters: new algorithms and results. *IEEE Trans Image Process* **4**, 499–502.
4. Huang TS, Yang GJ, Tang GY (1979) Fast two-dimensional median filtering algorithm. *IEEE Trans Acoust Speech Signal Process* **1**, 13–18.
5. Nodes TA, Gallagher Jr NC (1984) The output distribution of median type filters. *IEEE Trans Commun* **32**, 532–541.
6. Astola J, Kuosmanen P (1997) *Fundamentals of Nonlinear Digital Filtering*, CRC, Boca Raton.
7. Nikolova M (2004) A variational approach to remove outliers and impulse noise. *J Math Imaging Vis* **20**, 99–120.
8. Chan RH, Ho CW, Nikolova M (2005) Salt-and-pepper noise removal by median-type noise detector and edge-

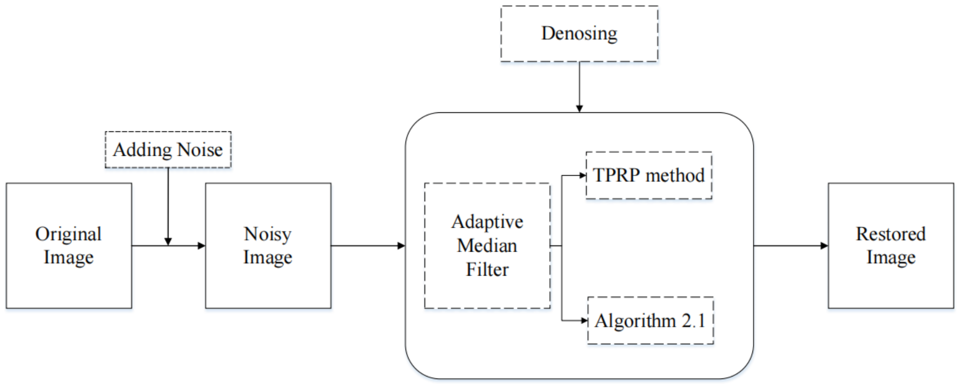

Fig. 1 Flow chart of our experiments.

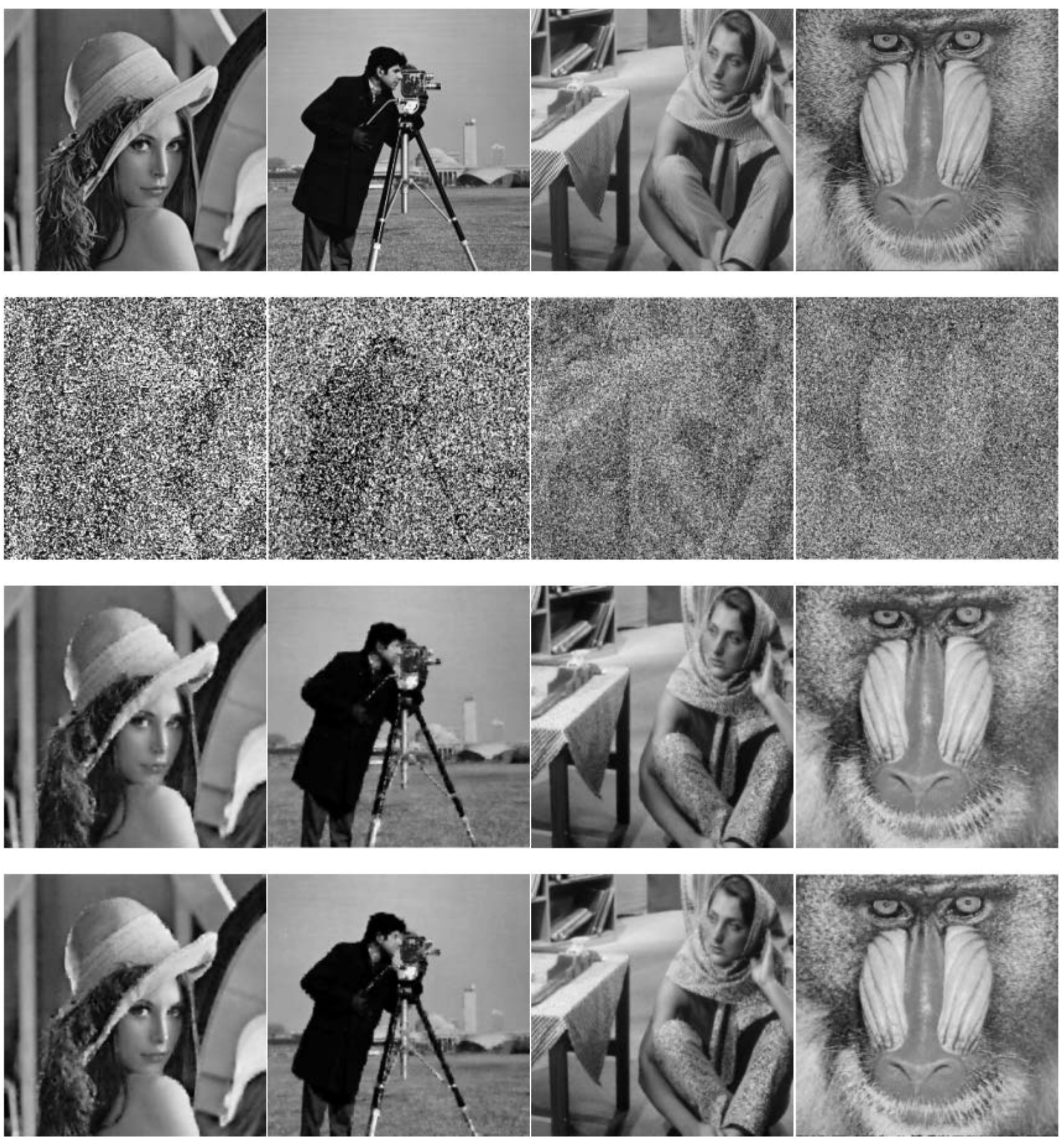

Fig. 2 From top to bottom: original images, noisy images with 0.7 the salt-and-pepper noise, the restorations obtained by minimizing $\mathscr{F}_\alpha$ with TPRP method and Algorithm 1, respectively.

preserving regularization. *IEEE Trans Image Process* **14**, 1479–1485.

9. Liu JK, Cao HS, Zhao YH, Zhang LQ (2021) A gradient-type iterative method for impulse noise removal. *Numer Linear Algebra with Appl* **28**, e2358.
10. Guo L, Zhao XL, Gu XM, Zhao YL, Zheng YB, Huang TZ (2021) Three dimensional fractional total variation regularized tensor optimized model for image deblurring. *Appl Math Comput* **404**, 126224.
11. Chan RH, Ho CW, Leung CY, Nikolova M (2005) Minimization of detail-preserving regularization functional by Newton's method with continuation. In: *Proceedings of IEEE International Conference on Image Processing*, Genova, Italy, pp 125–128.
12. Cai JF, Chan RH, Morini B (2007) Minimization of an edge-preserving regularization functional by conjugate gradient types methods. In: *Image Processing Based on Partial Differential Equations: Proceedings of the International Conference on PDE-based Image Processing and Related Inverse Problems*, Springer, Berlin, pp 109–122.
13. Dong Y, Chan RH (2007) A detection statistic for random-valued impulse noise. *IEEE Trans Image Process* **16**, 1112–1120.
14. Yin JH, Jian JB, Jiang XZ (2021) A generalized hybrid CGPM-based algorithm for solving large-scale convex constrained equations with applications to image restoration. *J Comput Appl Math* **391**, 113423.
15. Yu GH, Huang JH, Zhou Y (2010) A descent spectral conjugate gradient method for impulse noise removal. *Appl Math Lett* **23**, 555–560.
16. Cheng WY (2007) A two-term PRP-based descent method. *Numer Func Anal Opt* **28**, 1217–1230.
17. Huber PJ (1973) Robust regression: asymptotics, conjectures, and Monte Carlo. *Ann Stat* **1**, 799–821.
18. Polak E, Ribière G (1969) Note sur la convergence de méthodes de directions conjugées. *Rev Francaise Informat Recherche Opertionelle* **16**, 35–43.
19. Polyak BT (1969) The conjugate gradient method in extreme problems. *USSR Comp Math Math Phys* **9**, 94–112.
20. Bovik A (2000) *Handbook of Image and Video Processing*, Academic Press, New York.